# *Oral mRNA delivery using capsule-mediated gastrointestinal tissue injections*

Matter

CellPress

Article

# Oral mRNA delivery using capsule-mediated gastrointestinal tissue injections

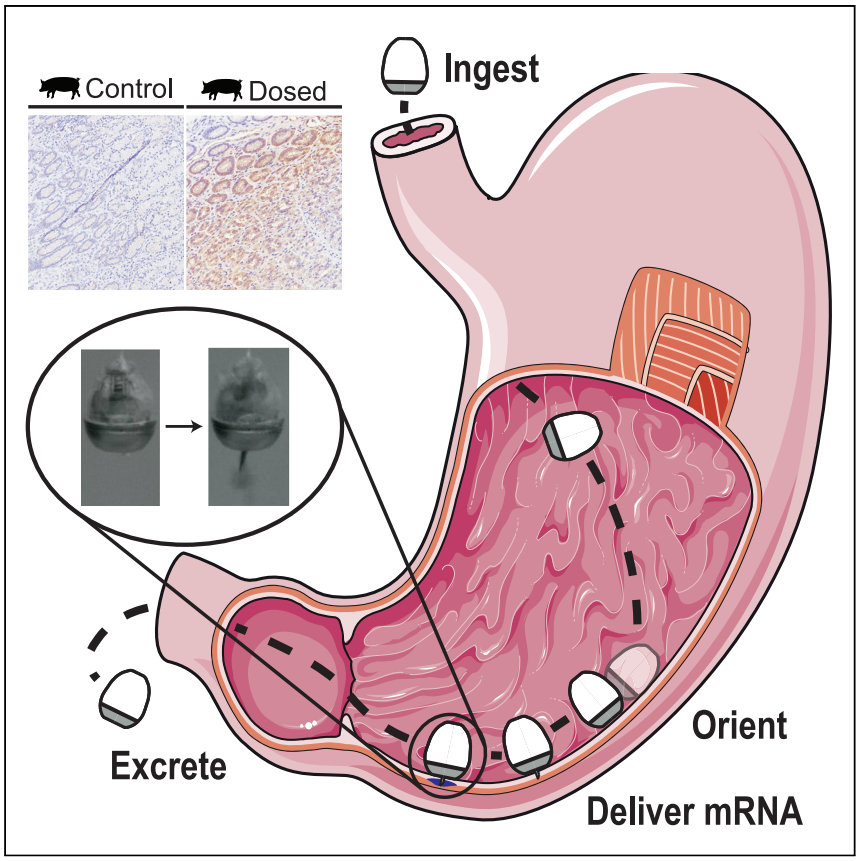


Alex Abramson, Ameya R. Kirtane, Yunhua Shi, ..., Brian Jensen, Robert Langer, Giovanni Traverso

rlanger@mit.edu (R.L.)
cgt20@mit.edu,
ctraverso@bwh.harvard.edu (G.T.)

## Highlights

Orally dosed milli-injector capsules enable nucleic acid delivery to swine stomachs

Branched hybrid poly(β-amino ester) mRNA NPs transfect cells with high efficiency

Systemic and gastric mRNA delivery is achieved using this formulation-device combo

Nucleic acid therapeutics and vaccines are only available as injectable formulations that generate discomfort and lead to low patient acceptance. To enable oral delivery, these therapeutics must avoid enzymatic degradation and bypass physical tissue barriers in the gastrointestinal tract. Here, the authors describe orally dosed pills capable of delivering nanoparticle formulations of nucleic acids with high transfection efficiencies via milli-needle injections into the gastric lining. This formulation-device combination results in gastric and systemic uptake in large and small animals, respectively.

4 **Demonstrate**
Proof-of-concept of performance with intended application/response

Abramson et al., Matter 5, 975–987
March 2, 2022 
https://doi.org/10.1016/j.matt.2021.12.022

Matter

CellPress

Article

# Oral mRNA delivery using capsule-mediated gastrointestinal tissue injections

Alex Abramson,[1,2,8,9] Ameya R. Kirtane,[1,2,3,8] Yunhua Shi,[1,2,3,8,10] Grace Zhong,[1,2,11] Joy E. Collins,[1,2,3] Siddartha Tamang,[1,2] Keiko Ishida,[1,2] Alison Hayward,[1,2,3,4] Jacob Wainer,[1,2,12] Netra Unni Rajesh,[1,2,13] Xiaoya Lu,[1,2,14] Yuan Gao,[1,2] Paramesh Karandikar,[1,2,15] Chaoyang Tang,[1,2] Aaron Lopes,[1,2] Aniket Wahane,[1,2,16] Daniel Reker,[2,3,17] Morten Revsgaard Frederiksen,[5,18] Brian Jensen,[5] Robert Langer,[1,2,6,7,*] and Giovanni Traverso[1,2,3,7,19,*]

## SUMMARY

**Nucleic acids are enabling a new generation of therapeutics and vaccines to treat and prevent a range of diseases. While these therapies have typically been limited to parenteral dosing, patients and clinicians prefer oral dosage forms. Furthermore, oral delivery enables local transfection of cells in the gastrointestinal tract not easily targeted via parenteral administration. To address these challenges, we synthesized and screened a library of branched hybrid poly(β-amino ester) mRNA nanoparticles for transfection efficiency; then we combined the highest performing formulations with ingestible milli-injector capsules capable of delivering formulations directly into gastric tissue. We validated the performance of formulations and devices in rodents and pigs, demonstrating protein translation in the delta, gastric, and parietal cells of the gastric mucosa, in addition to systemic uptake. We anticipate oral delivery of mRNA could facilitate rapid deployment of episodic interventions, such as vaccines, and support long-term therapies.**

## INTRODUCTION

Therapeutic nucleic acids, such as antisense oligonucleotides,[1] siRNA,[2] and mRNA,[3] have been used to treat and prevent a variety of diseases. For example, nucleic acid-based therapeutics have been shown to improve clinical outcomes in patients with hereditary transthyretin-mediated amyloidosis[4] and homozygous familial hypercholesterolemia.[5] In addition, experimental nucleic acid-based vaccines have recently been developed for cancer and Zika virus, and nucleic acid-based vaccines for COVID-19 have been approved for clinical use.[6–10] Because mRNA vaccines can be developed more rapidly than other vaccine types, nucleic acid-based therapeutics could play an important role in controlling pandemic diseases.[7,11]

Even though patients prefer oral dosage forms over injections,[12,13] nucleic acids are generally administered intravenously, intramuscularly, or subcutaneously because the gastrointestinal (GI) tract naturally prohibits biomacromolecule uptake. When administered orally, nucleic acids rapidly degrade after ingestion, thus limiting cellular permeation and reducing bioavailability.[14] Parenteral delivery methods enable rapid systemic uptake and ensure that therapies reach organs receiving large amounts of blood flow, such as the liver,[15] lungs,[16] and kidneys.[17] Oral administration methods could enable a preferred method of systemic uptake and would also allow for targeted delivery in the GI tract.

### Progress and potential

Nucleic acid therapeutics and vaccines, such as the COVID-19 vaccine, are only available as injectable formulations because these therapeutic molecules cannot survive passage through the gastrointestinal tract. Injectable formulations often result in low acceptance and adherence by patients because they cause discomfort and require a trained professional for administration. Here, we describe orally dosed pills capable of delivering nanoparticle formulations of nucleic acids with high transfection efficiencies. The pills achieve delivery via milli-needle injections into the gastric lining. Evidence from small and large animal studies demonstrates that this form of administration enables both gastric and systemic uptake and transfection.

To enhance GI uptake, target a specific organ, promote transfection, and/or prevent off-target effects, nucleic acid- and other macromolecule-based medications have often turned to permeation enhancers and specially designed nanoparticles.[18–21] Still, nucleic acid-based therapeutics continue to have low oral bioavailability. We and others have previously demonstrated that orally dosed robotic injection pills, which autonomously inject drugs into the lining of the GI tract, are capable of systemic delivery of macromolecule protein drugs in dose levels comparable with subcutaneous injection.[22–27] However, oral delivery of nucleic acids presents additional challenges and has yet to be demonstrated using this method. In this paper, we demonstrate the ability to directly inject mRNA encapsulated in branched polymer nanoparticles into the stomach submucosa via an orally administered capsule, bypassing the natural barriers present in the GI tract. We use evidence of protein translation in swine and mouse models to confirm effective transfection of the dosed mRNA.

## RESULTS

Our pill, which we call the self-orienting millimeter-scale applicator (SOMA), is capable of bypassing the degradative enzymes in the GI tract by delivering a formulation of medication directly into the vascularized layers of stomach tissue via a tissue injection.[22,26] By injecting the drug into the tissue, rather than relying on diffusion through the gastric mucus and mucosa, the pill is capable of delivering drugs with a wide range of molecular weights. To ensure the injection passes into the tissue, rather than into the gastric lumen, the pill utilizes a unique shape and density distribution to autonomously self-orient and predictably face the stomach wall. Similar to a leopard tortoise or a weeble-wobble toy, the pill only possesses one stable configuration in which the injection mechanism faces toward the tissue wall.[28] Once the pill self-orients, a hydration-triggered actuator releases a spring-based injection mechanism that propels a needle into the tissue and delivers a bolus of drug to the gastric submucosa. Earlier studies performed in swine and dogs demonstrated that our device can be ingested and can deliver small molecules, peptides, and monoclonal antibodies systemically via the stomach submucosa without generating a full thickness perforation or causing a GI obstruction.[22,26,29] This paper focuses on optimizing the SOMA system to address the unique challenges posed by nucleic acid delivery such as dose potency, transfection efficiency, and translation rates (Figure 1).

Oral capsules have greater volume restrictions than some parenteral dosage forms to facilitate ingestion and prevent GI obstruction: this limits drug loading. Since mRNA supports amplification of a protein molecule, mRNA-based formulations can be used to create potent vaccines and therapeutics. However, unlike current protein therapies, nucleic acids must be delivered intracellularly to realize their therapeutic benefits. To address the issues of dose size and intracellular uptake, we developed a potent nanoparticle for nucleic acid delivery and designed a formulation that was amenable to lyophilization, up-concentration, and filling into the SOMA device (Figure 1A). Specifically, we created libraries of branched and branched hybrid poly(β-amino ester) (PBAE) nanoparticles, which were used to encapsulate the mRNA. We then compared the transfection efficiency of mRNA delivered using our branched and branched hybrid PBAE nanoparticles to those that used linear PBAE nanoparticles. To measure transfection efficiency, we complexed the polymers with GFP-encoding plasmid DNA and measured protein expression using high-throughput flow cytometry (Figures 1B–1G). *In vitro* studies with multiple cell types showed that the top branched or branched hybrid PBAE nanoparticles transfected a greater percentage of cells than the linear PBAE nanoparticles. Branched hybrid PBAEs also potently delivered eGFP-encoding mRNA

[1]Department of Chemical Engineering, Massachusetts Institute of Technology, Cambridge, MA 02139, USA

[2]David H. Koch Institute for Integrative Cancer Research, Massachusetts Institute of Technology, Cambridge, MA 02139, USA

[3]Division of Gastroenterology, Hepatology, and Endoscopy, Brigham and Women's Hospital, Harvard Medical School, Boston, MA 02115, USA

[4]Division of Comparative Medicine, Massachusetts Institute of Technology, Cambridge, MA 02139, USA

[5]Global Research Technologies, Global Drug Discovery, and Device & Delivery Solutions, Novo Nordisk A/S, Maaloev, Denmark

[6]Institute for Medical Engineering and Science, Massachusetts Institute of Technology, Cambridge, MA 02139, USA

[7]Department of Mechanical Engineering, Massachusetts Institute of Technology, Cambridge, MA 02139, USA

[8]These authors contributed equally

[9]Present address: Stanford University, 443 Via Ortega, Stanford, CA 94305, USA

[10]Present address: The Charles Stark Draper Laboratory, 555 Technology Square, Cambridge, MA 02139, USA

[11]Present address: Stanford University, 443 Via Ortega, Stanford, CA 94305, USA

[12]Present address: Fractyl Laboratories, 17 Hartwell Ave., Lexington, MA 02421, USA

[13]Present address: Stanford University, 443 Via Ortega, Stanford, CA 94305, USA

[14]Present address: Johns Hopkins University, 720 Rutland Avenue, Baltimore, MD 21205, USA

[15]Present address: University of Massachusetts Chan Medical School, 55 Lake Avenue N, Worcester, MA 01655, USA

[16]Present address: University of Connecticut, 69 N Eagleville Rd, Storrs, CT 06269, USA

[17]Present address: Duke University, 101 Science Dr., CIEMAS RM, Durham, NC 27708, USA

[18]Present address: Orbex Space, Copenhagen, Denmark/Forres, UK

[19]Lead contact

*Correspondence: rlanger@mit.edu (R.L.), cgt20@mit.edu, ctraverso@bwh.harvard.edu (G.T.)

https://doi.org/10.1016/j.matt.2021.12.022

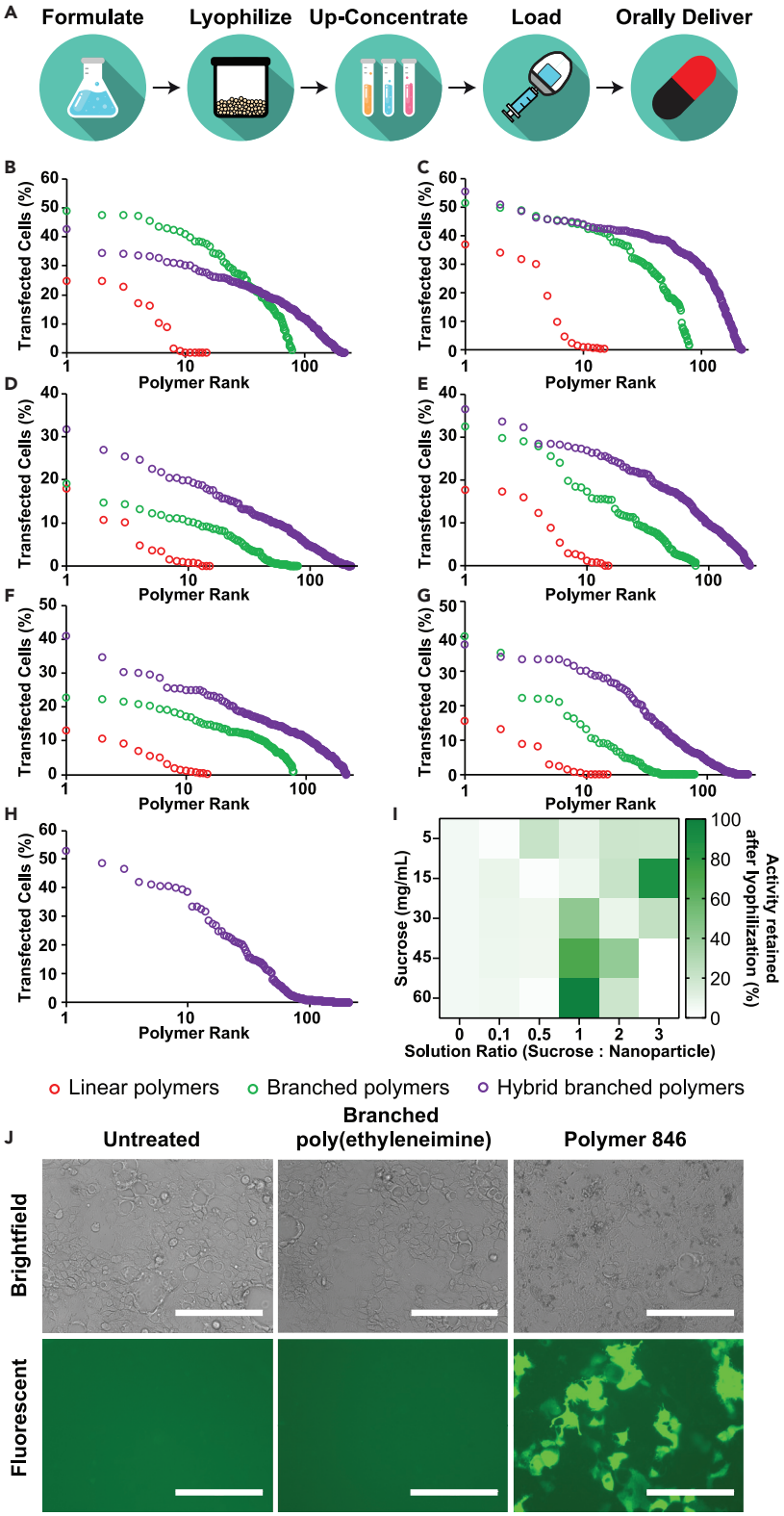
A
Formulate
Lyophilize
Up-Concentrate
Load
Orally Deliver
B
C
D
E
F
G
H
Transfected Cells (%)
Polymer Rank
I
Sucrose (mg/mL)
Solution Ratio (Sucrose : Nanoparticle)
Activity retained after lyophilization (%)
Linear polymers
Branched polymers
Hybrid branched polymers
J
Untreated
Branched poly(ethyleneimine)
Polymer 846
Brightfield
Fluorescent

**Figure 1. Transfection efficiency of branched hybrid polymer nanoparticles**
(A) Flow diagram of drug formulation and loading into an orally dosed device.
(B–G) *In vitro* transfection efficiency of plasmid DNA encapsulated in linear PBAE, branched PBAE, or hybrid branched PBAE nanoparticles in (B) HeLa, (C) Caco2, (D) mesenchymal stem, (E) PK15, (F) RAW, and (G) human aortic epithelial cells.
(H) *In vitro* transfection efficiency of mRNA encapsulated in hybrid branched PBAE nanoparticles in Caco2 cells.
(I) Transfection efficiency of GFP-encoding mRNA encapsulated in branched hybrid PBAE nanoparticles after lyophilization in Caco2 cells.
(J) Imaging of transfected Caco2 cells transfected with GFP-encoding mRNA. Scale bars, 200 μm.

into Caco2 cells. In fact, the transfection efficiency of one of the top hits (846) was substantially greater than branched polyethyleneimine, which is considered the gold standard gene carrier (Figures 1H and 1J). Cell viability studies are presented in Figures S1 and S2. Physicochemical characterization of the polymers and nanoparticles in the library is presented in Figures S1–S6. A description of the chemical composition of the polymers is presented in Table S1.

To increase the dose of mRNA that could be loaded into an orally dosed capsule, we lyophilized the nanoparticles and reconstituted them at a higher concentration. Lyophilization in the absence of a protectant led to a complete loss of transfection efficiency. However, adding sucrose in select concentrations led to a complete retention of transfection efficiency (Figure 1I) and allowed us to increase the concentration of nanoparticles by a factor of >100×. It should be noted that we used high quantities of sucrose to stabilize the nanoparticles during lyophilization (15–60× weight of nanoparticles), which is comparable with or lower than literature reported values for nucleic acid delivery systems.[30,31] Previous studies have shown that incorporation of surface active agents, such as poly(vinyl alcohol) or docusate sodium, may help reduce the amount of sugar during lyophilization of nanoparticles.[32,33] The use of non-ionic agents such as poly(vinyl alcohol) may be particularly beneficial for these nanoplexes. Despite the high quantity of sugar used, lyophilization allowed us to increase the concentration of the nanoparticles, making them amenable for our ingestible injector. Hence, with these potent nanoparticle formulations, we proceeded to *in vivo* studies. Physicochemical analyses of polymers and nanoparticles used in *in vivo* studies are shown in Table S1 and Figure S6.

We chose three top-hit polymers (846, 877, and 995) for *in vivo* evaluation based on their differential transfection ability *in vitro* and differences in the constituent branching agents used. Materials with differential constituent chemicals were chosen for two reasons. First, it is well established that *in vitro-in vivo* correlation in transfection is weak.[34–36] We wanted to maximize our ability to identify a material that enables *in vivo* transfection. Second, we wanted to evaluate if different chemical composition enabled cell-selective transfection, as has been reported in the field of lipid nanoparticles.[37,38] To determine the transfection efficiency of our formulations *in vivo*, we first administered nanoparticles made from polymer 877 to mice via a tail vein injection. We then compared the transfection efficiency of this intravenous administration method to the delivery of the mRNA nanoparticles via a direct injection to the stomach submucosa, mimicking the oral capsule delivery method we planned to use in swine (Figure 2A). In these experiments, we delivered 20 μg (100 μL) of mRNA encoding Cre recombinase enzyme (Cre) to genetically modified mice designed to produce tdTomato fluorescent protein in the presence of the enzyme. This allowed us to quantify total transfection efficiency and determine the cell types targeted using a stomach injection delivery method and compare it with intravenous injection.[39] We then harvested tissue samples 48 h after administration, which allowed enough time for Cre-mediated tdTomato

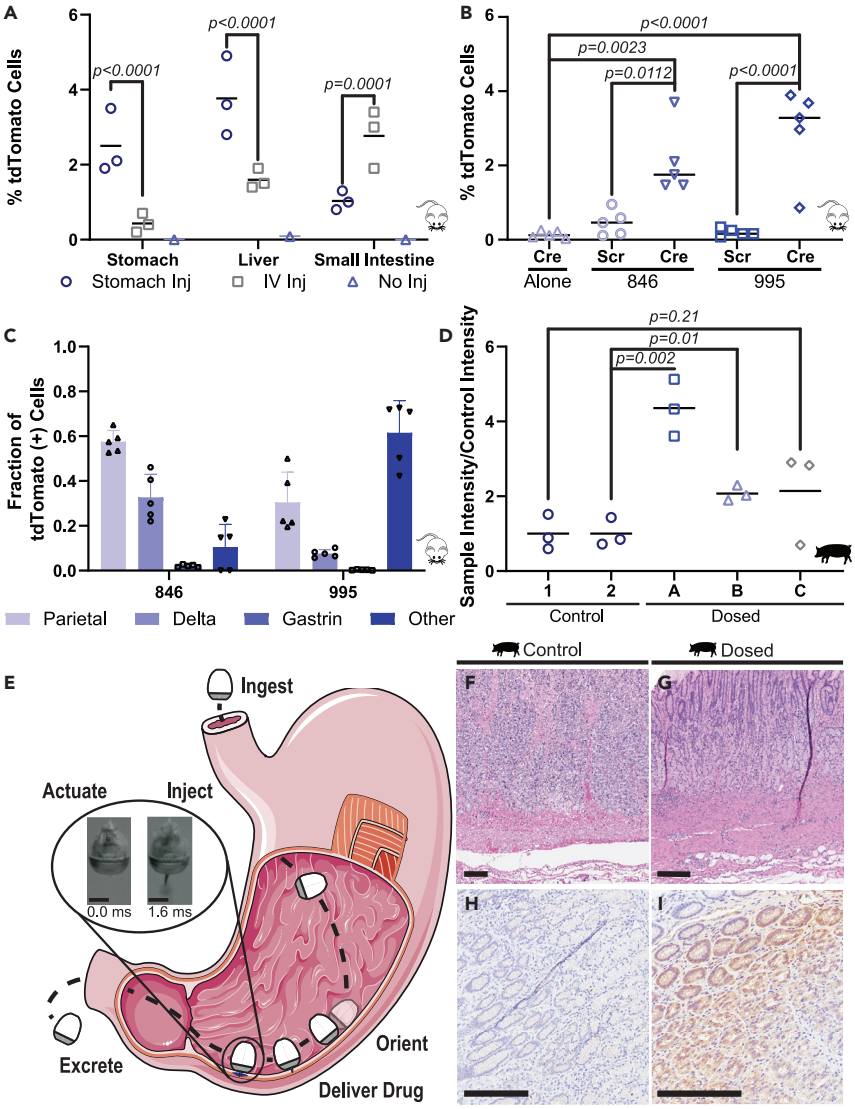


**Figure 2. *In vivo* delivery of mRNA to the stomach in mice and swine**

(A) Flow cytometry-based analysis of tdTomato expression in mice treated with 20 μg of Cre mRNA complexed with polymer 877 after a direct injection into the stomach submucosa, an intravenous (i.v.) injection into the tail vein, or no injection of mRNA in mice that produce tdTomato after exposure to Cre (n = 3). Mean ± SD, two-way ANOVA.

(B) Flow cytometry-based quantification of transfection efficiency of 20 μg of Cre mRNA complexed with polymer 846 or 995 in mice after a direct injection to the stomach submucosa compared with delivery of scrambled (Scr) mRNA nanoparticles or Cre mRNA alone (n = 5 per group, cells within group combined). Mean ± SD, one-way ANOVA.

(C) Flow cytometry-based analysis of the composition of tdTomato+ cells in the stomach in mice treated with gastric injection of Cre mRNA nanoparticles (n = 5 per group, cells within group combined). Mean ± SD.

(D) Quantification of western blot of swine stomach tissue after dosing with 150 μg of Cre mRNA (50 μg each in three capsules) encapsulated in polymer 846 via a direct injection to the stomach submucosa through an oral autoinjection pill administered via an overtube. This is compared with untreated tissue as a control. Dosed: n = 3 animals, 3 devices per animal in 3 tissue sites; control: n = 2 animals, 3 tissue sites per animal. (A and B) Run on gel with Ctrl 2. (C) Run on gel with Ctrl 1. Mean ± SD, multiple t tests.

(E) Schematic of device delivery and slow-motion capture of a prototype actuating while suspended in water *in vitro*. Scale bars, 5 mm.

**Figure 2. *Continued***
(F–I) (F and G) Hematoxylin and eosin-stained histology and (H and I) immunohistochemistry histology stained against Cre from a representative control swine and dosed swine B. The histology from the two other dosed swine is shown in Figure S7. Scale bars, 200 μm.

expression. Flow cytometry data demonstrated that mRNA delivery via stomach injection using formulation 877 resulted in a greater tdTomato expression in the stomach compared with delivery via a tail vein injection. In addition, systemic uptake via the stomach injection was confirmed by transfection of liver cells. In a follow-up experiment performed to determine the stomach cell types targeted during a direct stomach injection, we dosed mice with one of two other top-hit formulations, 846 or 995 (Figure 2B). As controls, we administered naked mRNA and nanoparticles made from the same polymers and loaded with scrambled mRNA via direct stomach injections. Mouse stomachs were collected and stained with antibodies specific to parietal cells, gastrin cells, and delta cells. Our data showed that the proportion of tdTomato+ cells in each cell group correlated with the cell populations in the stomach[40] and were unaffected by the polymer used (Figure 2C). We concluded that these nanoparticles were able to transfect cells in small animal models, and we then proceeded to dose large animal models.

To demonstrate the ability of our robotic injection capsule to deliver mRNA, we administered three SOMA pills, each containing 50 μg (80 μL) of the mRNA encoding for Cre encapsulated within nanoparticles made from polymer 846, to each of three swine. Previous histological studies of the SOMA capsule demonstrate that the pill delivers an injection of drug directly into the gastric submucosa, comparable with the direct gastric injections performed in the previous experiments in mice.[26] Because of a limitation in drug solubility to a formulation equivalent to 0.625 mg mRNA/mL (on account of the added sucrose) and a dose loading capacity of 80 μL of formulation in the SOMA pill, the dose scale-up from the mouse to the swine did not constitute a linear relative dose increase based on model size. However, the 150 μg delivered to the swine represents clinically relevant doses larger than both the Moderna and Pfizer mRNA COVID-19 vaccine doses of 100 and 30 μg, respectively. 24 h after dosing, we euthanized the swine and harvested tissue samples within a 1-cm radius of each injection site. In addition, we collected liver tissue adjacent to the portal vein entrance. As a control, we harvested tissue from swine that were not dosed with any formulation. We observed the presence of Cre in the stomach via a western blot in two of the three swine (Figure 2D). In the third swine, the western blot quantification did not demonstrate a statistically significant change from the control. A histological evaluation was performed with hematoxylin and eosin staining (Figures 2E and 2F; see Figure S7) without evidence of toxicity. Immunohistochemistry staining (Figures 2G and 2H; see Figure S7) confirmed the presence of Cre in the stomach tissue of the same two animals that demonstrated translation in the western blot quantification. We saw no significant Cre expression in the liver via a western blot or an immunohistochemistry stained against Cre (see Figure S8). The differences in protein translation efficiency among the swine were likely due to several factors, including physiological and behavioral animal variation, as well as variability in the manual dose loading and tissue harvesting processes. Because we visualized the injection of the nanoparticle formulation into the stomach lining of all three swine, the absence of Cre translation in one of the three swine was more likely due to variations in the transfection of the mRNA particles into cells rather than a device malfunction.

## DISCUSSION

These findings suggest that directly injecting mRNA, as well as other nucleic acids, into the lining of the gut via an orally administered device may be a feasible method to deliver these therapeutic molecules to the GI tissue. The gastric mucosa plays an

important role in mucosal immunity for gastric diseases, such as those caused by *Helicobacter pylori*; moreover, using these capsules to systemically deliver nucleic acids via uptake through the gastric vein could enable our oral delivery system to produce systemic immune responses similar to traditional intramuscular injections.[41,42] Future work assessing the mucosal immunity through B cell and T cell responses could help determine if immune responses are focused in the stomach or disseminated through the GI tract and the rest of the body. While the capsule presented here is designed specifically for gastric injections, capsules designed to inject substances into other areas of the GI tract, such as the oral cavity, esophagus, small intestine, and colon, may also allow other organs and mucosal surfaces in the GI tract to be targeted.[23,24,43,44] The SOMA device used in this study has been designed to circumvent enzymatic degradation, reduce absorption limitations associated with oral biomacromolecule delivery,[45] reduce the risk of full-thickness perforation and obstruction linked to sharp or large ingested objects,[46] and eliminate the pain and stigma associated with parenteral administration.[13] Validation in additional large animal models and humans, however, is still required to assess the clinical safety and efficacy of this device. We used a branched hybrid PBAE nanoparticle in our experiments, but other polymer and lipid nanoparticles might also be compatible with our system.[47] Importantly, nanoparticle optimization, which could reduce the effects of nucleic acid degradation *in vivo* after tissue injection, was not performed; additional studies are warranted to further optimize the dosing efficiency of these nanoparticle formulations. While we did not see Cre translation in the livers of the dosed swine, we did see evidence of Cre translation in the mouse model, which suggests that higher doses of our formulation may be needed for systemic uptake in large animal models. To realize the full potential of this system, studies using therapeutic nucleic acids, such as mRNA vaccines, rather than the model nucleic acids used in this study, should be performed. Still, this pill is a promising development for oral nucleic acid delivery technologies and could lead to a higher quality of life among patient populations[13] and ultimately improve health outcomes.

## EXPERIMENTAL PROCEDURES

### Resource availability

#### *Lead contact*

Further information and requests for resources and reagents should be directed to and will be fulfilled by the lead contact, Giovanni Traverso (cgt20@mit.edu, ctraverso@bwh.harvard.edu).

#### *Materials availability*

All protocols describing the synthesis of the materials used in this research are provided in the manuscript or the supplementary materials.

#### *Data and code availability*

The authors declare that the data supporting the findings of this study are available within the paper and its supplementary information files. The authors declare that there was no code generated during the study.

### Materials

Dimethyl sulfoxide (DMSO), tris(2-amino ethylamine), 2,2′ ethylenedioxy bis(ethylamine), cysteamine, *N*-methylethylenediamine, 5-amino-1-pentanol, 3-amino-1,2-propanediol, and 3-amino-1-propanol were obtained from Sigma-Aldrich. 1,4-Butanediol diacrylate, 1,6-hexanediol diacrylate, and 1-(3-aminopropyl)-4-methypiperazine were obtained from Alfa Aesar. 1,3-Propanediol diacrylate was purchased from Monomer-Polymer and Dajac Labs. 2,4,6-Trinitrobenzylsulfonic acid (TNBSA) was

purchased from Thermo Fisher Scientific. CleanCap eGFP and Cre mRNA were purchased from TriLink BioTechnologies (San Diego, USA).

### Synthesis and characterization of PBAEs

To prepare the linear polymers, the amine and diacrylate were weighed in an 8-mL glass vial. The amount of amine and diacrylate used in the reaction is listed in Table S1. A stir bar was placed in the glass vial and the vial was placed on a magnetic stir plate at 90°C. The reaction was allowed to proceed overnight to yield the linear polymers.[48–50] Select polymers were end capped with an excess of amine.[51] For this reaction, the linear polymers were dissolved in DMSO at a concentration of 100 mg/mL, then 1-(3-aminopropyl)-4-methypiperazine was added to this solution. The mixture was placed on a shaker at room temperature for 2 h.

To prepare branched and branched hybrid polymers, the linear polymers were dissolved in DMSO at a concentration of 166.7 mg/mL. Branching agents were dissolved in DMSO at a concentration of 100 mg/mL. The branching agent solution and the polymer solution were mixed in a 4-mL glass vial in volume ratios described in Table S1. DMSO was added to this mixture, which brought the total volume to 0.58 mL. The samples were placed on a shaker at room temperature for 24 h. To synthesize the branched polymers, one linear polymer was used for each reaction. For the branched hybrid polymers, two linear polymers were used. Following the branching reaction, the polymers were end capped using 1-(3-aminopropyl)-4-methypiperazine as described above.

To determine the progression of the branching reaction, we used two orthogonal methods: one method measured the consumption of the terminal acrylate groups in the polymer; the second method evaluated the incorporation of the branching agent into the polymer. To evaluate the consumption of the acrylate groups in the branching reaction, we mixed the linear polymers with the branching agent using a method identical to the one described for polymer synthesis. At various times, the reaction mixture was analyzed using $^{1}$H-NMR (Brucker) and the area under the curve of the acrylate peak was measured. Linear polymers without any branching agent were used as the control (Figure S3). To confirm the progression of the branching reaction, we also measured the amount of unreacted branching agent in the reaction mixture. To perform this analysis, the linear polymers were mixed with the branching agent using a method identical to that used for the synthesis of the polymers. At various times, 0.1 M sodium bicarbonate (pH 8.5) was added to the reaction mixture, which led to the precipitation of both the polymer and the reacted branching agent. The mixture was centrifuged and the supernatant containing unreacted branching agent was collected and stored at −20°C until further analysis. The concentration of amines (branching agent) in the samples was measured using a TNBSA assay (Thermo Fisher Scientific, 28997) according to the manufacturer's protocol (Figure S4). For each assay, a standard curve of the branching agent in question was prepared to ascertain the linearity of the assay.

### Synthesis and physicochemical characterization of PBAE nanoparticles

To synthesize the nanoparticles, DMSO-based solutions of the polymers were diluted in 25 mM sodium acetate buffer (pH 3.8) to a concentration of 2 mg/mL. Nucleic acid (plasmid DNA or mRNA) was diluted in the same buffer to a concentration of 0.02 mg/mL. Equal volumes of the polymer and nucleic acid solutions were mixed by adding the polymer solution to the solution of the nucleic acid and pipetting the mixture 15 to 20 times. The mixture was allowed to stand for 10 min to ensure complete formation of the nanoplexes.[52] The nanoplexes were diluted in deionized

water before analysis. Size and zeta potential of the nanoparticles were determined using a Zeta NanoZS machine (Malvern) (Figure S5).

Encapsulation efficiency was determined as described by Kaczmarek et al. with some changes.[16] Nanoparticles were prepared as described above. Following the 10-min standing, the nanoparticles were centrifuged at 12,000 rpm for 15 min. The supernatant was discarded to remove the unencapsulated mRNA and the nanoparticle pellet was dispersed in Tris-EDTA buffer (pH 8). The polymer-mRNA complex was disrupted by incubating with heparin (10 mg/mL, Tris-EDTA buffer) for 15 min at 37°C. RiboGreen reagent was added to the samples and fluorescence was measured. Standards of known concentrations were treated the same way and were used to produce a calibration curve.

### High-throughput analysis of the *in vitro* transfection efficiency of PBAE nanoparticles

We tested the ability of nanoparticles to transfect a variety of cells *in vitro* using high-throughput flow cytometry. We tested the nanoparticles in RAW cells (mouse macrophage), PK15 cells (pig kidney), HeLa cells (human cervical cancer), human mesenchymal stem cells, Caco2 cells (human colon cancer cells), and primary human aortic endothelial cells. Cells were plated in a 96-well plate 1 day before transfection. For all cells except Caco2 cells, 10,000 cells were plated in each well. Twenty-five thousand cells were seeded in each well for Caco2 cells. On the day of the experiment, polymers dissolved in DMSO were diluted to 2 mg/mL in 25 mM acetate buffer. The polymer solution was mixed with a solution of plasmid DNA or mRNA (0.02 mg/mL in 25 mM acetate buffer; sfGFP-N1 plasmid [Addgene], or eGFP CleanCap mRNA [TriLink BioTechnologies]) to form the nanoparticles. The nanoparticles were added to the cells and diluted with serum-free medium to achieve a plasmid concentration of 1 μg/mL. After 4.5 h, the treatments were replaced with complete medium. Twenty-four hours later, cells were collected using appropriate dissociation medium (trypsin for Caco2 cells, TrypLE for all other cells) and analyzed using flow cytometry on an Intellicyt iQue high-throughput flow cytometer. Data in Figure 1 are the median values reported from three biologically independent experiments. Each circle represents an individual polymer.

We measured the cytotoxicity of plasmid-loaded nanoparticles. Plasmid or mRNA nanoparticles were prepared and incubated with HeLa/Caco2 cells for 4 h. After 4 h, the treatments were removed and the cells were incubated with fresh medium for 24 h. The viability of cells was measured using an Alamar Blue assay according to the manufacturer's protocol. Cell viability is represented as a percentage of untreated cells. Data are presented in Figures S1 and S2. Some polymers did show cytotoxicity; however, this was a small fraction of the polymers described here.

### Nanoparticle lyophilization

The goal of these experiments was to design a formulation of nanoparticles that retains its transfection efficiency following lyophilization. To enable protection, we decided to use a commonly used cryoprotectant: sucrose. Nanoparticles were prepared as described above by mixing polymer 846 and mRNA. Sucrose solutions (5, 15, 30, 45, and 60 mg/mL) in acetate buffer were added to the nanoparticle dispersion at volume ratios of 0.1:1, 0.5:1, 1:1, 2:1, and 3:1. The suspensions were frozen at −80°C and lyophilized (Labconco). Following lyophilization, the nanoparticles were dispersed in a mixture of water and serum-free medium to ensure isotonicity. Following lyophilization, since the majority of the formulation contains sucrose, it appeared to be a translucent/opaque pellet. Following reconstitution in medium, the appearance was clear and indistinguishable from freshly prepared nanoparticles.

Nanoparticles were added to cells and incubated for 4.5 h, after which the treatments were replaced with serum-containing medium. Twenty-four hours later, transfection efficiency was assessed using high-throughput flow cytometry as described above. Freshly prepared nanoparticles were used as positive controls. Transfection efficiency of lyophilized nanoparticles is expressed relative to that of the freshly prepared nanoparticles in Figure 1H.

### *In vivo* mice studies

All animal experiments were approved by and performed in accordance with the MIT Committee on Animal Care. Four- to 6-week-old B6.Cg-Gt(ROSA)26Sor$^{tm9(CAG-tdTomato)Hze}$/J mice were purchased from Jackson Laboratory and were allowed 1 week to acclimate to their new environment. Mice received preemptive analgesia before surgery. Mice were given buprenorphine sustained release at 1 mg/kg subcutaneously (s.c.) before recovery. They were given one dose of meloxicam 1–2 mg/kg s.c. during surgical prep period. If they appeared to be in pain, meloxicam was continued daily for the next 2–3 days. Mice were anesthetized with isoflurane in an induction box and maintained on isoflurane for the duration of the procedure via a nose cone (2–3% isoflurane in oxygen for maintenance). The animal was placed in dorsal recumbency and the abdomen was shaved from just cranial to the xiphoid process to just caudal to the umbilical area. The skin was aseptically prepared with alternating cycles of betadine or similar scrub and 70% ethyl alcohol. The animal was maintained on a heating blanket (warm water circulating) and monitored for depth of anesthesia by quality of respiratory effort and response to toe pinch. A 1-cm incision was made on the ventral midline through both the skin and the linea alba. Using atraumatic forceps and sterile cotton tip applicators, we stabilized the area of interest (stomach or small intestine). Using a 30-gauge needle, we injected the biological molecule of interest suspended in PBS into the subserosal side targeting the submucosal space. We then delivered 100 μL of fluid. To deliver this amount, we performed up to 10 injections per mouse in different locations of the tissue. Before recovery, mice were given sterile warm 0.9% NaCl s.c. at 20 mL/kg. Mice were maintained on a heating blanket and given warm fluids subcutaneously as well as recovered in a cage on a heating blanket. The abdominal wall was closed with 5-0 PDS or similar absorbable monofilament using a simple interrupted pattern. The skin was closed with a wound clip. Mice were fed alfalfa-free food a week before and after surgery to prevent any background fluorescence. Forty-eight hours after surgery, mice were euthanized via $CO_2$ asphyxiation. The tissue was harvested and sent for histology and fluorescence-activated cell sorting.

### *In vivo* swine studies

All animal experiments were approved by and performed in accordance with the MIT Committee on Animal Care. We administered the mRNA-loaded robotic injection pill to female Yorkshire swine, 60–75 kg (Tufts, Grafton, USA). Twenty-four hours before administration, we placed the swine on a liquid diet and fasted the swine overnight. We sedated the swine with an intramuscular injection of Telazol (tiletamine/zolazepam) (5 mg/kg), xylazine (2 mg/kg), and atropine (0.05 mg/kg), and, if needed, supplemental isoflurane (1–2% in oxygen). We placed an orogastric tube, with guidance of a gastric endoscope, in the esophagus to ease the passage of the device. The robotic injection capsules were passed through the tube and dropped into the insufflated stomach from a height of 5–7 cm. The devices were left to actuate and sit in the stomach for up to 2 h after placement. Then the devices were removed from the stomach of the swine and the metal device pieces were recovered and washed for future experiments. A rough map of the injection locations was made using the gastric endoscope. In addition, gastric clips were placed around the sites of injection, and methylene blue dye was added to the injection

formulation to potentially allow us to spot the injection location at a later time. Twenty-four hours after administration, the swine were euthanized. Stomach tissue was harvested from the injection site locations. Methylene blue dye was no longer visible in the stomach tissue. Liver tissue was harvested from a location adjacent to the portal vein. The tissue was then sent for histology and western blot. Western blot and immunohistochemistry used the Anti-Cre Recombinase antibody clone 2D8 at a concentration of 1:500 (MAB3120, Sigma-Aldrich). Western blot also used the HRP goat anti-rabbit IgG H&L from Abcam at a concentration of 1:2,000.

### Flow cytometry

Tissue samples were isolated from euthanized animals using a 4-μm biopsy punch and incubated in DMEM medium supplied with 1 mg/mL collagenase type IV (Thermo Fisher Scientific) and 20 μg/mL DNAseI (Thermo Fisher Scientific) in a 37°C shaker (450 rpm) for 1 h. After digestion, single cells were obtained through a 70-μm cell strainer and stained with Cy5 NHS ester (GE Healthcare)-conjugated [Lys]-Bombesin at a ratio of 1:250. After Cytofix/Cytoperm (BD) cell fixation was performed according to standard protocol, each sample was stained with a primary antibody and a secondary antibody at 4°C for 1 h. The sample was then analyzed using an LSR II (BD). Data were analyzed using FlowJo. An SSTR polyclonal antibody at a concentration of 1:250 purchased from Thermo Fisher Scientific (PA3-16736) was used to stain delta cells. An anti-α1 sodium potassium ATPase-FITC antibody at a concentration of 1:100 was purchased from Santa Cruz Biotechnology (Dallas, USA) (sc-48345 FITC) and used to stain parietal cells. [Lys]-Bombesin (Sigma-Aldrich, B1647, St. Louis, USA) conjugated to Cy-5 (GE Healthcare Life Sciences, PA15101) was used to stain gastric cells. A goat anti-rabbit IgG, APC-Cy-7 antibody (Santa Cruz Biotechnology, sc-3847) was used as a secondary antibody for detecting parietal cells.

### Statistical analysis

No data were excluded from the analysis. Student's t tests or one- or two-way ANOVA were performed using Prism version 7.0 (GraphPad) or Microsoft Excel (Microsoft). A value of $p < 0.05$ was considered statistically significant. Figure captions and text describe the number of replicates used in each study. Figure captions define the center line and error bars present in the plots.

## SUPPLEMENTAL INFORMATION

Supplemental information can be found online at https://doi.org/10.1016/j.matt.2021.12.022.

## ACKNOWLEDGMENTS

We thank J. Haupt and M. Jamiel for help with the *in vivo* porcine work. We thank the Koch Institute for Integrative Cancer Research at MIT's Swanson Biotechnology Center high-throughput sciences core (J. Cheah and C. Sellinger), Hope Babette Tang (1983) Histology Core, Swanson Biotechnology Center Flow Cytometry Core, and Preclinical Modeling, Imaging & Testing core. We are grateful to all members of the Langer and Traverso laboratories and Novo Nordisk for their expertise and discussions around biologic drug delivery. We acknowledge Servier medical art and vecteezy.com for use of their vector images in the figures. This work was funded in part by a grant from Novo Nordisk, NIH grant no. EB-000244. A.A. was supported in part by the NSF GRFP fellowship. A.R.K. is grateful to PhRMA foundation postdoctoral fellowship for financial support. G.T. was supported in part by the Division of Gastroenterology, Brigham and Woman's Hospital and the Department of

Mechanical Engineering, MIT and the Karl van Tassel (1925) Career Development Professorship, MIT.

## AUTHOR CONTRIBUTIONS

A.A., A.R.K., and Y.S. designed the study. A.R.K., G.Z., P.K., C.T., A.L., A.W., and D.R. developed and tested the polymers and nanoparticle formulations. A.A., J.W., X.L., M.R.F., and B.J. developed the robotic injection device. Y.S. performed the flow cytometry and western blot analysis. A.A., J.C., S.T., K.I., A.H., N.R., X.L., and Y.G. performed in vivo experiments. R.L. and G.T. designed, supervised, reviewed the data, and edited the manuscript. All authors edited and contributed to the manuscript.

## DECLARATION OF INTERESTS

A.A., J.W., X.L., M.R.F., B.J., R.L., Y.G., and G.T. are co-inventors on multiple patent applications describing oral biologic drug delivery. A.R.K., G.Z., D.R., R.L., and G.T. are co-inventors on multiple patent applications describing nucleic acid delivery. A.A. reports receiving consulting fees from Eli Lilly. A.A., R.L., and G.T. report receiving consulting fees from Novo Nordisk. M.R.F. and B.J. are employees of Novo Nordisk. D.R. acts as a consultant for the pharmaceutical and biotechnology industry and a mentor for the German Accelerator Life Sciences. Complete details of all relationships for profit and not for profit for G.T. can found at the following link: https://www.dropbox.com/sh/szi7vnr4a2ajb56/AABs5N5i0q9AfT1IqIJAE-T5a?dl=0. For a list of entities with which R.L. is involved, compensated or uncompensated, see https://www.dropbox.com/s/ntcfggbr44bew5q/Langer%20COI.pdf?dl=0.

Received: August 9, 2021
Revised: October 13, 2021
Accepted: December 6, 2021
Published: January 31, 2022

## REFERENCES

1. Geary, R.S., Norris, D., Yu, R., and Bennett, C.F. (2015). Pharmacokinetics, biodistribution and cell uptake of antisense oligonucleotides. Adv. Drug Deliv. Rev. *87*, 46–51.

2. Whitehead, K.A., Langer, R., and Anderson, D.G. (2009). Knocking down barriers: advances in siRNA delivery. Nat. Rev. Drug Discov. *8*, 129–138.

3. Sahin, U., Karikó, K., and Türeci, Ö. (2014). MRNA-based therapeutics—developing a new class of drugs. Nat. Rev. Drug Discov. *13*, 759–780.

4. Adams, D., Gonzalez-Duarte, A., O'Riordan, W.D., Yang, C.-C., Ueda, M., Kristen, A.V., Tournev, I., Schmidt, H.H., Coelho, T., Berk, J.L., et al. (2018). Patisiran, an RNAi therapeutic, for hereditary transthyretin amyloidosis. N Engl J Med *379*, 11–21.

5. Raal, F.J., Santos, R.D., Blom, D.J., Marais, A.D., Charng, M.-J., Cromwell, W.C., Lachmann, R.H., Gaudet, D., Tan, J.L., Chasan-Taber, S., et al. (2010). Mipomersen, an apolipoprotein B synthesis inhibitor, for lowering of LDL cholesterol concentrations in patients with homozygous familial hypercholesterolaemia: a randomised, double-blind, placebo-controlled trial. Lancet *375*, 998–1006.

6. Pardi, N., Hogan, M.J., Porter, F.W., and Weissman, D. (2018). mRNA vaccines—a new era in vaccinology. Nat. Rev. Drug Discov. *17*, 261–279.

7. Thanh Le, T., Andreadakis, Z., Kumar, A., Gómez Román, R., Tollefsen, S., Saville, M., and Mayhew, S. (2020). The COVID-19 vaccine development landscape. Nat. Rev. Drug Discov. *19*, 305–306.

8. Richner, J.M., Himansu, S., Dowd, K.A., Butler, S.L., Salazar, V., Fox, J.M., Julander, J.G., Tang, W.W., Shresta, S., Pierson, T.C., et al. (2017). Modified mRNA vaccines protect against Zika virus infection. Cell *168*, 1114–1125.e10.

9. Baden, L.R., El Sahly, H.M., Essink, B., Kotloff, K., Frey, S., Novak, R., Diemert, D., Spector, S.A., Rouphael, N., Creech, C.B., et al. (2021). Efficacy and safety of the mRNA-1273 SARS-CoV-2 vaccine. N Engl J Med *384*, 403–416.

10. Sahin, U., Oehm, P., Derhovanessian, E., Jabulowsky, R.A., Vormehr, M., Gold, M., Maurus, D., Schwarck-Kokarakis, D., Kuhn, A.N., Omokoko, T., et al. (2020). An RNA vaccine drives immunity in checkpoint-inhibitor-treated melanoma. Nature *585*, 107–112.

11. Gates, B. (2020). Responding to COVID-19—a once-in-a-century pandemic? N. Engl. J. Med. *382*, 1677–1679.

12. Abramson, A., Halperin, F., Kim, J., and Traverso, G. (2019). Quantifying the value of orally delivered biologic therapies: a cost-effectiveness analysis of oral semaglutide. J Pharm Sci *108*, 3138–3145.

13. Boye, K.S., Matza, L.S., Walter, K.N., Van Brunt, K., Palsgrove, A.C., and Tynan, A. (2011). Utilities and disutilities for attributes of injectable treatments for type 2 diabetes. Eur. J. Heal. Econ. *12*, 219–230.

14. Kriegel, C., Attarwala, H., and Amiji, M. (2013). Multi-compartmental oral delivery systems for nucleic acid therapy in the gastrointestinal tract. Adv. Drug Deliv. Rev. *65*, 891–901.

15. Lorenzer, C., Dirin, M., Winkler, A.M., Baumann, V., and Winkler, J. (2015). Going beyond the liver: progress and challenges of targeted delivery of siRNA therapeutics. J. Control Release *203*, 1–15.

16. Kaczmarek, J.C., Patel, A.K., Kauffman, K.J., Fenton, O.S., Webber, M.J., Heartlein, M.W., DeRosa, F., and Anderson, D.G. (2016). Polymer–lipid nanoparticles for systemic

delivery of mRNA to the lungs. Angew Chem - Int. Ed. *55*, 13808–13812.

17. Zuckerman, J.E., Choi, C.H.J., Han, H., and Davis, M.E. (2012). Polycation-siRNA nanoparticles can disassemble at the kidney glomerular basement membrane. Proc. Natl. Acad. Sci. U S A *109*, 3137–3142.

18. O'Driscoll, C.M., Bernkop-Schnürch, A., Friedl, J.D., Préat, V., and Jannin, V. (2019). Oral delivery of non-viral nucleic acid-based therapeutics—do we have the guts for this? Eur. J. Pharm. Sci. *133*, 190–204.

19. Aouadi, M., Tesz, G.J., Nicoloro, S.M., Wang, M., Chouinard, M., Soto, E., Ostroff, G.R., and Czech, M.P. (2009). Orally delivered siRNA targeting macrophage Map4k4 suppresses systemic inflammation. Nature *458*, 1180–1184.

20. Nurunnabi, M., Lee, S.-A., Revuri, V., Hwang, Y.H., Kang, S.H., Lee, M., Cho, S., Cho, K.J., Byun, Y., Bae, Y.H., et al. (2017). Oral delivery of a therapeutic gene encoding glucagon-like peptide 1 to treat high fat diet-induced diabetes. J. Control Release *268*, 305–313.

21. Cheng, C.J., Tietjen, G.T., Saucier-Sawyer, J.K., and Saltzman, W.M. (2015). A holistic approach to targeting disease with polymeric nanoparticles. Nat. Rev. Drug Discov. *14*, 239–247.

22. Abramson, A., Caffarel-Salvador, E., Khang, M., Dellal, D., Silverstein, D., Gao, Y., Frederiksen, M.R., Vegge, A., Hubálek, F., Water, J.J., et al. (2019). An ingestible self-orienting system for oral delivery of macromolecules. Science (80-) *363*, 611–615.

23. Abramson, A., Caffarel-Salvador, E., Soares, V., Minahan, D., Tian, R.Y., Lu, X., Dellal, D., Gao, Y., Kim, S., Wainer, J., et al. (2019). A luminal unfolding microneedle injector for oral delivery of macromolecules. Nat. Med. *25*, 1512–1518.

24. Hashim, M., Korupolu, R., Syed, B., Horlen, K., Beraki, S., Karamchedu, P., Dhalla, A.K., Ruffy, R., and Imran, M. (2019). Jejunal wall delivery of insulin via an ingestible capsule in anesthetized swine—a pharmacokinetic and pharmacodynamic study. Pharmacol. Res. Perspect. *7*, e00522.

25. Dhalla, A.K., Al-Shamsie, Z., Beraki, S., Dasari, A., Fung, L.C., Fusaro, L., Garapaty, A., Gutierrez, B., Gratta, D., Hashim, M., et al. (2021). A robotic pill for oral delivery of biotherapeutics: safety, tolerability, and performance in healthy subjects. Drug Deliv. Transl. Res. *12*, 294–305.

26. Abramson, A., Frederiksen, M.R., Vegge, A., Jensen, B., Poulsen, M., Mouridsen, B., Jespersen, M.O., Kirk, R.K., Windum, J., Hubálek, F., et al. (2021). Oral delivery of systemic monoclonal antibodies, peptides and small molecules using gastric auto-injectors. Nat. Biotechnol. *2021*, 1–7.

27. Søgaard, P.P., Lind, M., Christiansen, C.R., Petersson, K., Clauss, A., Caffarel-Salvador, E., and Marzio, L. (2021). Future perspectives of oral delivery of next generation therapies for treatment of skin diseases. Pharm *13*, 1722.

28. Domokos, G., and Várkonyi, P.L. (2008). Geometry and self-righting of turtles. Proc. Biol. Sci. *275*, 11–17.

29. Abramson, A., Dellal, D., Kong, Y.L., Zhou, J., Gao, Y., Collins, J., Tamang, S., Wainer, J., McManus, R., Hayward, A., et al. (2020). Ingestible transiently anchoring electronics for microstimulation and conductive signaling. Sci. Adv. *6*, eaaz0127.

30. Guerrero-Cázares, H., Tzeng, S.Y., Young, N.P., Abutaleb, A.O., Quiñones-Hinojosa, A., and Green, J.J. (2014). Biodegradable polymeric nanoparticles show high efficacy and specificity at DNA delivery to human glioblastoma in vitro and in vivo. ACS Nano *8*, 5141–5153.

31. Ball, R.L., Bajaj, P., and Whitehead, K.A. (2016). Achieving long-term stability of lipid nanoparticles: examining the effect of pH, temperature, and lyophilization. Int. J. Nanomedicine *12*, 305–315.

32. Wendorf, J., Singh, M., Chesko, J., Kazzaz, J., Soewanan, E., Ugozzoli, M., and O'Hagan, D. (2006). A practical approach to the use of nanoparticles for vaccine delivery. J. Pharm. Sci. *95*, 2738–2750.

33. Chacon, M., Molpeceres, J., Berges, L., Guzman, M., and Aberturas, M.R. (1999). Stability and freeze-drying of cyclosporine loaded poly(D,L lactide-glycolide) carriers. Eur. J. Pharm. Sci. *8*, 99–107.

34. Dahlman, J.E., Kauffman, K.J., Xing, Y., Shaw, T.E., Mir, F.F., Dlott, C.C., Langer, R., Anderson, D.G., and Wang, E.T. (2017). Barcoded nanoparticles for high throughput in vivo discovery of targeted therapeutics. Proc. Natl. Acad. Sci. U S A *114*, 2060–2065.

35. Hajj, K.A., Ball, R.L., Deluty, S.B., Singh, S.R., Strelkova, D., Knapp, C.M., and Whitehead, K.A. (2019). Branched-tail lipid nanoparticles potently deliver mRNA in vivo due to enhanced ionization at endosomal pH. Small *15*, 1805097.

36. Whitehead, K.A., Matthews, J., Chang, P.H., Niroui, F., Dorkin, J.R., Severgnini, M., and Anderson, D.G. (2012). In vitro–in vivo translation of lipid nanoparticles for hepatocellular siRNA delivery. ACS Nano *6*, 6922–6929.

37. Liu, S., Cheng, Q., Wei, T., Yu, X., Johnson, L.T., Farbiak, L., and Siegwart, D.J. (2021). Membrane-destabilizing ionizable phospholipids for organ-selective mRNA delivery and CRISPR–Cas gene editing. Nat. Mater. *205*, 701–710.

38. Fenton, O.S., Kauffman, K.J., Kaczmarek, J.C., McClellan, R.L., Jhunjhunwala, S., Tibbitt, M.W., Zeng, M.D., Appel, E.A., Dorkin, J.R., Mir, F.F., et al. (2017). Synthesis and biological evaluation of ionizable lipid materials for the in vivo delivery of messenger RNA to B lymphocytes. Adv. Mater. *29*, 1606944.

39. Kauffman, K.J., Oberli, M.A., Dorkin, J.R., Hurtado, J.E., Kaczmarek, J.C., Bhadani, S., Wyckoff, J., Langer, R., Jaklenec, A., and Anderson, D.G. (2018). Rapid, single-cell analysis and discovery of vectored mRNA transfection in vivo with a loxP-flanked tdTomato reporter mouse. Mol. Ther. - Nucleic Acids *10*, 55–63.

40. Choi, E., Roland, J.T., Barlow, B.J., O'Neal, R., Rich, A.E., Nam, K.T., Shi, C., and Goldenring, J.R. (2014). Cell lineage distribution atlas of the human stomach reveals heterogeneous gland populations in the gastric antrum. Gut *63*, 1711–1720.

41. Holmgren, J., and Czerkinsky, C. (2005). Mucosal immunity and vaccines. Nat Med *114*, S45–S53.

42. Nie, S., and Yuan, Y. (2020). The role of gastric mucosal immunity in gastric diseases. J Immunol Res *2020*. https://doi.org/10.1155/2020/7927054.

43. Babaee, S., Pajovic, S., Kirtane, A.R., Shi, J., Caffarel-Salvador, E., Hess, K., Collins, J.E., Tamang, S., Wahane, A.V., Hayward, A.M., et al. (2019). Temperature-responsive biometamaterials for gastrointestinal applications. Sci Transl Med *11*, eaau8581.

44. Aran, K., Chooljian, M., Paredes, J., Rafi, M., Lee, K., Kim, A.Y., An, J., Yau, J.F., Chum, H., Conboy, I., et al. (2017). An oral microjet vaccination system elicits antibody production in rabbits. Sci. Transl. Med. *9*. https://doi.org/10.1126/scitranslmed.aaf6413.

45. Moroz, E., Matoori, S., and Leroux, J.-C. (2016). Oral delivery of macromolecular drugs: where we are after almost 100 years of attempts. Adv. Drug Deliv. Rev. *101*, 108–121.

46. Velitchkov, N.G., Grigorov, G.I., Losanoff, J.E., and Kjossev, K.T. (1996). Ingested foreign bodies of the gastrointestinal tract: retrospective analysis of 542 cases. World J. Surg. *20*, 1001–1005.

47. Kowalski, P.S., Rudra, A., Miao, L., and Anderson, D.G. (2019). Delivering the messenger: advances in technologies for therapeutic mRNA delivery. Mol. Ther. *27*, 710–728.

48. Green, J.J., Shi, J., Chiu, E., Leshchiner, E.S., Langer, R., and Anderson, D.G. (2006). Biodegradable polymeric vectors for gene delivery to human endothelial cells. Bioconjug. Chem. *17*, 1162–1169.

49. Akinc, A., Anderson, D.G., Lynn, D.M., and Langer, R. (2003). Synthesis of poly(β-amino ester)s optimized for highly effective gene delivery. Bioconjug. Chem. *14*, 979–988.

50. Anderson, D.G., Peng, W., Akinc, A., Hossain, N., Kohn, A., Padera, R., Langer, R., and Sawicki, J.A. (2004). A polymer library approach to suicide gene therapy for cancer. Proc. Natl. Acad. Sci. U S A *101*, 16028–16033.

51. Zugates, G.T., Peng, W., Zumbuehl, A., Jhunjhunwala, S., Huang, Y.-H., Langer, R., Sawicki, J.A., and Anderson, D.G. (2007). Rapid optimization of gene delivery by parallel end-modification of poly(β-amino ester)s. Mol. Ther. *15*, 1306–1312.

52. Green, J.J., Langer, R., and Anderson, D.G. (2008). A combinatorial polymer library approach yields insight into nonviral gene delivery. Acc. Chem. Res. *41*, 749–759.